CHARACTERIZATION OF THE TEXTURE OF HEAVILY DEFORMED METAL-METAL COMPOSITES WITH ACOUSTIC MICROSCOPY

R. B. Thompson, Y. Li, and W. A. Spitzig

Ames Laboratory and College of Engineering
Iowa State University
Ames, Iowa 50011, USA

G. A. D. Briggs and A. Fagan

Department of Metallurgy and Science of Materials
Oxford University
Oxford, England

J. Kushibiki

College of Engineering
Tohoku University
Sendai, Japan

INTRODUCTION

Composite materials are playing an increasingly important role as structural components. Familiar motivations for their use include the ability to achieve high ratios of strength to weight, tailored elastic stiffnesses, damage tolerance, etc. A new class of these materials which has recently received considerable attention for structural applications is the heavily deformed metal-metal composites[1,2]. Through extensive deformation processing of two ductile components, e.g. Nb dendrites in a Cu matrix, a fine, highly aligned, reinforced structure is produced. These heavily deformed metal-metal composites have been found to exhibit large mechanical strength in combination with high thermal and electrical conductivities at elevated temperatures[3,4]. In attempting to understand the mechanisms leading to these superior properties, an experimental determination of the microstructure developed during the deformation processing was undertaken. One aspect is the texture, or preferred grain orientation, developed during the deformation.

The preparation of these materials utilizes a casting procedure to produce, for the case of a Cu-Nb composite, an array of Nb dendrites in a copper matrix. Subsequent extrusion or rolling breaks up the dendrites and aligns them into long, ribbon-like filaments or platelets for the case of rod or plate material respectively. Figure 1 illustrates a typical microstructure for the case of Cu-Nb plate material. For the large reductions in area which produce the most interesting properties, the dimensions and separations of the Nb reinforcements are less than a micron. The crystallographic texture of the filaments and matrix are believed to jointly play a strong role in determining the mechanical properties by determining those directions along which easy dislocation motion can occur.

Review of Progress in Quantitative Nondestructive Evaluation, Vol. 9
Edited by D.O. Thompson and D.E. Chimenti
Plenum Press, New York, 1990

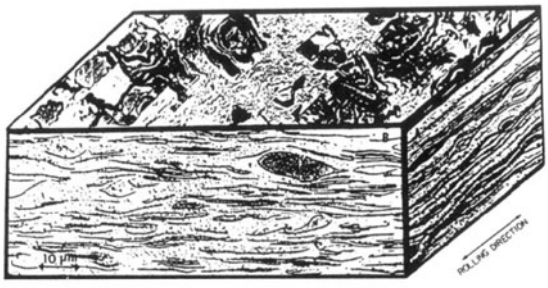

$\eta_e = 5.0$

Fig. 1. Micrograph of heavily deformed, Cu-20% Nb plate

It has been found that the strengthening is heavily dependent on the draw ratio η, defined as

$$\eta = \ln(A_o/A) \qquad (1)$$

where A_o is the initial and A is the final cross-sectional area. As η increases, the dendrite spacing decreases while the ultimate tensile strength increases rapidly, as illustrated in Fig. 2. The reason for the high technological interest in these materials is the fact that strengths comparable to those of high strength steels are approached while retaining a significant fraction of the thermal and electrical conductivities of copper.

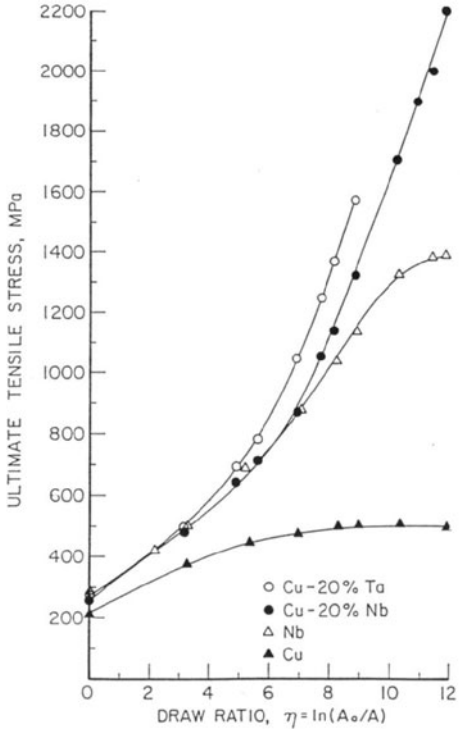

Fig. 2. Strength of heavily deformed metal-metal composite as a function of draw ratio

A variety of means are available for characterizing texture. Analysis of x-ray diffraction pole figures is the most familiar. However, difficulties have been reported in two phase materials, such as these aligned composites, because of the dependence of x-ray absorption on angle[5]. Another alternative, neutron diffraction, should be less susceptible to such problems but requires highly specialized sources and instrumentation. Each of these techniques samples a large number of grains. At the other extreme, diffraction patterns observed in focussed electron beam instruments such as transmission or scanning electron microscopes can determine the orientations of individual grains. The texture (distribution of grain orientations) can be built up by examining a large number of grains, but the numbers required to achieve the appropriate statistical accuracy may imply a quite tedious measurement.

In this paper, an alternate approach is considered. By measuring the angular dependence of the ultrasonic wave speed, one can obtain information on the crystallite orientations in a relatively simple fashion. Furthermore, by implementing this measurement with a high resolution acoustic microscope, it is possible to gain the information on a small volume of material with dimensions on the order of mm's. Here such a technique is used to study the development of texture in heavily deformed Cu-Nb and Cu-Ta composites.

THEORY

There are two sources of anisotropy in the microstructure shown in Fig. 1. The platelike structure of the niobium ribbons will introduce a geometrical anisotropy even if the copper and niobium are isotropic. In addition, any preferred crystalline texture in the copper or niobium will introduce additional anisotropy. Because of the thin, platelike structure of the niobium ribbons, we would expect little geometrically induced anisotropy in the plane of the plate. As a first approximation, that source of anisotropy will be neglected in this paper.

Consider then the anisotropy induced by the preferred anisotropy of the crystallites. The texture of a polycrytalline metal is defined by a crystallite orientation distribution function (CODF), $w(\theta,\psi,\phi)$, which defines the probability that a particular crystallite will have an orientation defined by the Euler angles θ,ψ,ϕ with respect to the axes of the plate. The CODF is usually parameterized by expanding it as a series of generalized Legendre functions, Z_{lmn}. Using the notation of Roe[6],

$$w(\zeta,\psi,\phi) = \sum_{l=0}^{\infty} \sum_{m=-l}^{l} \sum_{n=-l}^{l} W_{lmn} Z_{lmn}(\zeta) e^{-im\psi} e^{-in\phi} \qquad (2)$$

where the W_{lmn} are the orientation distribution coefficients (ODC's) and $\zeta = \cos\theta$.

In acoustic characterization of texture, one relies on functional relationships between the ODC's and the elastic constants. General arguments show that, when one attempts to express an anisotropic tensor property of rank r in terms of the texture, only coefficients with $l \leq r$ will be involved. Since the elastic constants are a fourth rank tensor, only ODC's with $l \leq 4$ can be studied by an ultrasonic approach. When the crystallites have cubic symmetry, further conditions cause many of the ODC's to vanish, and the only independent coefficients are W_{400}, W_{420}, and W_{440}. W_{000} also has a nonzero constant value determined by normalization requirements and is independent of texture.

For a single phased, polycrystalline aggregate, Sayers[7] has used these ideas to show that the angular dependence of the Rayleigh wave speed is equal to

$$V_R = V_R^\circ + \frac{c^\circ}{2\rho V_R^\circ}\{-2.26W_{400} + 8.75W_{420}\cos 2\theta + 0.89W_{440}\cos 4\theta\} \quad (3)$$

where V_R° is the Rayleigh velocity in the absence of texture, ρ is the density, c° is the elastic anisotropy, and the numerical factors pertain to a material with Poisson's ratio equal to 1/4. In these calculations, the Voigt procedure for obtaining polycrystalline elastic constants was utilized.

As a first approximation for a two-phased material, we have assumed that in each term, the factor $c^\circ W_{lmn}$ can be replaced by (1-p) c°(Cu) W(Cu) + pc°(Nb) W(Nb) where p is the volume fraction of the Nb and c° and W are the elastic anisotropy and ODC values for the material indicated in parentheses. This replacement follows from the notion that, in the Voigt approximation, the aggregate elastic stiffnesses are equal to the volume average of the local elastic stiffness. A similar expression applies to the case of Ta reinforcements.

Examination of the numerical values of the elastic anisotropy of both Nb or Ta show that they are less than that of Cu. Moreover, those materials occupy volume fractions of less than 20% of the composites studied. Hence the texture of reinforcing elements is believed to have only a small effect on the anisotropy of the Rayleigh velocity. In this work, that effect will be neglected. We thus interpret our Rayleigh wave velocity using Eq. (3), with the term in brackets multiplied by the factor (1-p) to account for the fraction of the material that is Cu.

MEASUREMENT TECHNIQUE

The samples were examined in a cylindrically focussed acoustic microscope and the Rayleigh wave velocity, as a function of angle, was inferred from the V(Z) data as described below[8]. Consider the highly focussed acoustic beam from a cylindrical lens which illuminates the sample through a water droplet. The signal from the sample will be dominated by energy propagating along two ray paths. In one, the energy is specularly reflected from the sample surface. In the second, the energy is incident at the critical angle for Rayleigh wave excitation on the sample surface. It then propagates along the surface as a Rayleigh wave and then leaks back through the water to the lens. The output is determined by the relative phases of these two contributions. As the distance between the focal point of the lens and the sample surface changes, the relative phases of these rays will also change, leading to a series of oscillations in a plot of acoustic signal versus the defocus Z. The Rayleigh wave velocity can be determined from the period of these oscillations.

If the lens were axially symmetric, the measured response would be an average of the velocities of Rayleigh waves propagating on all directions on the sample surface. However, when a cylindrical lens is used, the velocity is determined for waves propagating in a single direction perpendicular to the generating elements of the lens. Rotation of the lens about the Z-axis and repeating the V(Z) measurement at a series of orientations allows the angular dependence of the Rayleigh velocity to be inferred.

In this work, cylindrically focussed microscopes at Oxford University in Oxford, England, and Tohoku University in Sendai, Japan, were used. The former was used in a series of preliminary experiments whereas the numerical data repeated in this paper was obtained with the latter. A measurement frequency of 150 MHz was employed. The long axis of the lens was on the order of a mm while the nominal width of the spot size in the focal plan was 7 μm.

SAMPLES

Two alloys were studied: a copper-20 volume percent niobium alloy (Cu-20% Nb) and a copper-20 volume percent tantalum alloy (Cu-20% Ta). In each case, the appropriate stoichiometric mixture was first cast to form a composite with dendrites of Nb (or Ta) in a copper matrix. The samples were then heavily deformed by rolling into plates.

Seventeen samples were fabricated, as defined in Table I. Pure copper and niobium were rolled to several reduction levels to provide a reference for the effect of deformation on the texture of those constituents. One set of Cu-20% Nb and one set of Cu-20% Ta samples were then fabricated with a variety of draw ratios known to produce substantial strengthening.

The determination of the Rayleigh wave velocity in an acoustic microscope depends on an interference mechanism, and, the result is sensitive to the topography of the surface. In preparation for the acoustic microscopy measurements, the samples were mounted in a standard plastic metallurgical mount and polished to an optical finish.

DATA

Measurements of the angular dependence of the Rayleigh velocity on all of the pure copper and pure niobium specimens produced unsatisfactory data. On some, the form of the V(Z) response was such that reliable estimates of the Rayleigh velocity could not be obtained. On others, estimates of the Rayleigh velocity were obtained, but plots of velocity versus angle did not follow the functional form predicted by Eq. (3). Similar comments apply to the measurements on the as-cast composites ($\eta = 0$).

In contrast, the data on all the heavily deformed composites conformed with theoretical expectations. Figure 3 illustrates this by showing the Cu-20% Nb data for the highest and lowest draw ratios considered. Also shown is the result of least squares fits to the functional form

$$V_R = V_o + A\cos(2\theta - X_o) + B\cos(4\theta - X_o). \qquad (4)$$

Table I. Samples

Pure Copper		Pure Niobium	
h (mm)	η	h (mm)	η
60.96	0	60.96	0
1.6	3.6	1.6	3.6
0.79	4.3	0.76	4.4
0.30	5.3	0.38	5.1

Cu-20% Nb		Cu-20% Ta	
h (mm)	η	h (mm)	η
60.96	0	60.96	0
1.6	3.6	1.6	3.6
0.84	4.3	0.77	4.4
0.43	5.0	0.38	5.1
0.28	5.4		

h is the plate thickness, with 60.96 mm being the as cast value.

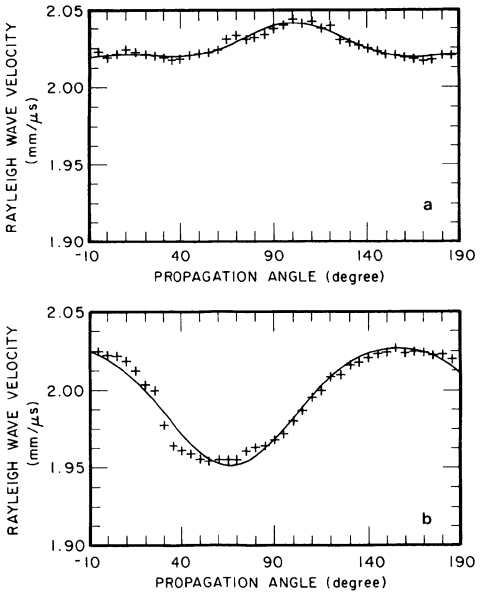

Fig. 3. Angular dependence of Rayleigh wave speed in Cu-20% Nb. (a) $\eta = 3.6$, (b) $\eta = 5.4$.

In these fits, the value of X_o, as well as A, B, and V_o, was adjustable since sample alignment had not been carefully controlled. However, no physical significance was attached to its value, which was simply a measure of the orientation of the sample with respect to the coordinate system of the microscope. Table II presents the values of V_o, A and B obtained from the fit. Figure 4 presents plots of V_o, and A versus η for both of the materials studied.

INTERPRETATION

Examination of Fig. 4 shows that both materials show similar trends with deformation: V_o decreases while A increases. In each case, the Cu-20% Nb experiences greater changes, with the values at high deformation approaching those of the Cu-20% Ta. Assuming that these changes are due to modifications of the texture of the copper, as implied by the above discussion, the following interpretation is consistent with the data. Suppose that the texture in the Cu-20% Ta had reached a nearly constant value before the draw ratio $\eta = 3.5$ had been reached, as suggested by the nearly constant value of V_o and A during subsequent deformation. It would then follow that the texture changes in Cu-20% Nb were not as well developed at that point, since significant change did

Table II. Data

Material	η	V_o (mm/μsec)	A (mm/μsec)	B (mm/μsec)
	3.6	2.0265	.0099	-.0043
Cu-20% Nb	4.3	2.0182	.0186	.0001
	5.0	2.0008	.0465	-.0059
	5.4	1.9935	.0383	-.0042
	3.6	1.9895	.0365	-.0012
Cu-20% Ta	4.4	1.9876	.0418	-.0053
	5.1	1.9851	.0418	-.0019

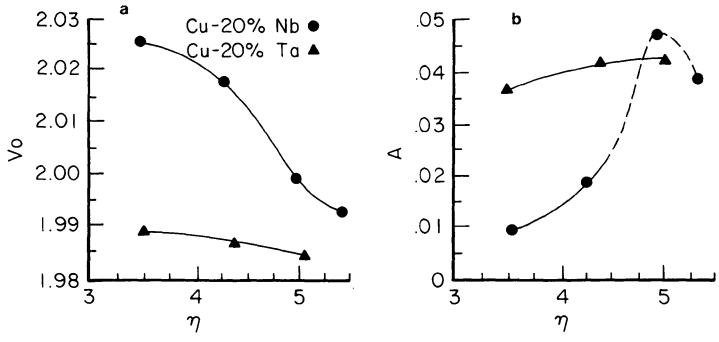

Fig. 4. Variation of Rayleigh wave parameters with deformation
(a) Average velocity, V_o
(b) Two-fold variation, A

occur in the range $3.5 < \eta < 5.5$. This behavior could be a result of the greater stiffness of Ta fibers with respect to Nb fibers, forcing more deformation to be born by the Cu matrix at lower deformations in Ta reinforced materials.

Comparison of the terms in Eqs. (3) and (4) provides a procedure to obtain the ODC's from the data. Assuming that W_{420} and W_{440} are of the same order of magnitude, Eq. (3) implies that B is an order of magnitude smaller than A. This is confirmed by the data. However, analysis of the errors suggests that attempts to infer W_{440} from B would be unreliable because of the small size of B, so this has not been attempted. The assumptions discussed above lead to the following two relations for W_{400} and W_{420}.

$$\delta W_{400}(Cu) = \frac{-2\rho V_o \delta V_o}{2.26(1-p)\ C^\circ(Cu)} \qquad (5a)$$

$$W_{420}(Cu) = \frac{2\rho V_o A}{8.75(1-p)C^\circ(Cu)} \qquad (5b)$$

Eq. (5a) shows only a relationship between changes in W_{400} and changes in V_o since the approximation in the analysis would render theoretical attempts to predict V_R° inaccurate. Table III presents the results of applying Eqs. (5) to the experimental data of Table II. For each material, the change in W_{400} is measured with respect to the sample having the lowest deformation ($\eta = 3.6$).

It is of interest to see how these results might compare to candidate textures. Table IV presented the expected values of the ODC's for certain ideal textures. The first three are classical textures

Table III. Estimated ODC's

MATERIAL	η	δW_{400}	W_{420}
Cu-20% Nb	3.6	---	-.0005
	4.3	-.0016	-.0009
	5.0	-.0048	-.0023
	5.4	-.0062	-.0019
Cu-20% Ta	3.6	---	-.0013
	4.4	-.0003	-.0015
	5.1	-.0006	-.0015

Table IV. ODC's of Candidate Texture

TEXTURE	W_{400}	W_{420}	W_{440}
{110} <112>: Classical, Low Deformation	-0.0078	-0.0083	-0.0109
{112} <111>: Classical, High Deformation	-0.0078	+0.0083	-0.0109
{100} <001>: Recrystallization	+0.0313	0	+0.0187
{112} <110>: TEM Observations	-0.0078	-0.0083	-0.0109

commonly found in copper plate. The fourth is a texture that has been identified in diffraction experiments on these materials in a transmission election microscope.

Comparison of the experimental predictions of Table III with ODC's of the ideal candidate textures in Table IV suggests that neither {112} <111> or {100} <001> textures are present in large quantities since they would require that W_{420} vanish or have an opposite sign from the data. The data is not able to distinguish the remaining two textures. It is encouraging that the experimental predictions in the most heavily deformed sample are of the same order, but less than the ODC's of these ideal textures.

CONCLUSIONS

A cylindrically focussed, scanning acoustic microscope, has been used to study the anisotropy of the Rayleigh wave speed in heavily deformed, metal-metal composites. The results are interpreted in terms of changes in the texture of the copper matrix induced by deformation. Numerical values are consistent with standard deformation textures. It would be useful to re-analyze the data after generalizing the theory to take into account the geometrical sources of the anisotropy.

ACKNOWLEDGEMENT

The Ames Laboratory is operated for the U.S. Department of Energy by Iowa State University under Contract No. W-7405-ENG-82. This work was supported by the Director of Energy Research, Office of Basic Energy Sciences.

REFERENCES

1. J. D. Verhoeven, F. A. Schmidt, E. D. Gibson, W. A. Spitzig, J. of Metals 38, 20 (1986).
2. W. A. Spitzig, A. R. Pelton, F. C. Laabs, Acta Met. 35, 2427 (1987).
3. W. A. Spitzig, Scripta Met. 23, 1177 (1989).
4. W. A. Spitzig, P. D. Krotz, Acta Met. 36, 1709 (1988).
5. H. J. Bunge, "Model Calculations of Youngs Modulus in two-phase composites," presented in Symposium on Modelling of Anisotropic Material Bahavior, 1988 TMS Fall Meeting, September 25-29, 1988, Chicago, IL.
6. R. -J. Roe, J. Appl. Phys., 36, 2024 (1965).
7. C. M. Sayers, "Angular Dependence of the Rayleigh Surface Wave Velocity in Polycrystalline Metals with Small Anistropy," Proc. Roy. Soc. Lond. A400, 175 (1985).
8. G. A. D. Briggs, An Introduction to Scanning Acoustic Microscopy, Royal Microscopical Society Microscopy Handbook 17 (Oxford University Press, Oxford, 1985).